

Modular Compilation for Quantum Chiplet Architectures

Mingyoung Jessica Jeng*

mingyoungjeng@u.northwestern.edu
Northwestern University
Evanston, Illinois, USA

Michael Gavrincea[†]

mgav@mit.edu
MIT Lincoln Laboratory
Lexington, MA, USA
Northwestern University
Evanston, Illinois, USA

Nikola Vuk Maruszewski*

nikola@u.northwestern.edu
Northwestern University
Evanston, Illinois, USA

Kaitlin N. Smith

kns@northwestern.edu
Northwestern University
Evanston, Illinois, USA

Connor Selna

ConnorSelna2021@u.northwestern.edu
Northwestern University
Evanston, Illinois, USA

Nikos Hardavellas

nikos@northwestern.edu
Northwestern University
Evanston, Illinois, USA

Abstract

As quantum computing technology matures, industry is adopting modular quantum architectures to keep quantum scaling on the projected path and meet performance targets. However, the complexity of chiplet-based quantum devices, coupled with their growing size, presents an imminent scalability challenge for quantum compilation. Contemporary compilation methods are not well-suited to chiplet architectures – in particular, existing qubit allocation methods are often unable to contend with inter-chiplet links, which don’t necessarily support a universal basis gate set. Furthermore, existing methods of logical-to-physical qubit placement, swap insertion (routing), unitary synthesis, and/or optimization, are typically not designed for qubit links of significantly varying latency or fidelity. In this work, we propose SEQC, a hierarchical parallelized compilation pipeline optimized for chiplet-based quantum systems, including several novel methods for qubit placement, qubit routing, and circuit optimization. SEQC attains a 9.3% average increase in circuit fidelity (up to 49.99%). Additionally, owing to its ability to parallelize compilation, SEQC achieves 3.27× faster compilation on average (up to 6.74×) over a chiplet-unaware Qiskit baseline.

Keywords

Quantum computing, quantum compilation, modular architectures.

1 Introduction

Classical computer systems, through the decades of their existence, have become increasingly distributed. Physical, technological, and economic constraints have prevented single “monolithic” systems from scaling to the point that they could meet the demand for high performance and yet remain practical. Today, distributed architectures are prevalent, and their latest renditions, from cloud computing to chiplet-based digital processors, are ubiquitous.

We postulate that quantum computing is on a similar path. While improvements in superconducting quantum hardware have led to the debut of processors with 1000+ qubits [13], practical implementations of quantum computation will require millions of physical qubits [35]. The number of qubits required by a quantum algorithm,

the depth of the algorithm (i.e., execution time or gate count on the critical path), the auxiliary and syndrome qubits required to reach sufficiently low error rates, and the size of qubits with all control hardware, all suggest that many more qubits are required than are likely to fit in a single die [49]. The overhead for error correction, cooling, dilution, control systems, I/O lines, challenges associated with verification and adequate chip thermalization, and realistic resources such as lossy waveguides, limited qubit fabrication yields as qubit capacity grows [45], and finite chip sizes, make the prospect of a single “monolithic” quantum processor very expensive or entirely unrealistic by current standards. These constraints force large-scale quantum systems to adopt a physically distributed architecture.

We are already observing signs of this shift. Recent developments in quantum chip linking, including flip-chip architectures [15] and low-loss coaxial cables [32], suggest that modular designs are the most viable for scaling [45]. Many contemporary or upcoming leading quantum systems adopt chiplet-based modular quantum processors, for example using high-bandwidth quantum links between nearest-neighbor quantum chiplets (e.g., carrier-chip couplers in Rigetti Aspen-M [42, 15], or m-couplers in IBM Crossbill [14, 27]), or lower-fidelity, lower-bandwidth, but longer-distance flexible coupling of discrete chips (e.g., l-couplers in IBM Flamingo [14, 27]), or a combination of the above (e.g., c-, m-, and l-couplers in IBM Starling [27]), or multi-chip connectivity through tunable couplers and routing chips [12]. Most major companies have set their sights at modular designs to meet quantum scaling targets in practical ways, and modular quantum processors dominate their latest roadmaps [18, 17, 40].

Unfortunately, current compilation infrastructure does not support quantum interconnect heterogeneity. The mapping of a quantum program’s logical quantum gates into the native gates supported by the underlying quantum processor, and the mapping of logical qubits to the physical qubits of the quantum hardware, largely determine the number and type of native quantum gates required for the computation, the circuit depth, and its execution time—long programs may not complete successfully as qubits decohere. Different mappings can result in vastly different compiled quantum circuits, with diverse characteristics along all these axes. These details of efficiency can make or break an algorithm in today’s noisy intermediate-scale quantum systems (NISQ) era, so

*These authors contributed equally to this work.

[†]All work performed while at Northwestern University prior to change of affiliation.

quantum compilers aggressively optimize for all of them. To make matters more challenging, each qubit, coupler, and gate have diverse error profiles that are highly variable both spatially and temporally [46, 30, 8]. Unlike classical compilation that is done only once for a given architecture, quantum programs must be recompiled every time before execution¹, as the ideal physical qubits to target change between runs. So, quantum compilers today are faced with the daunting task of optimizing quantum programs across multiple dimensions with often conflicting demands, in a continuously changing environment. Coupled with the hardness of synthesizing unitaries (which is exponential in the number of qubits) and the need for quick and frequent compilation, modern quantum compilers have no option other than to rely on heuristics to perform the task. These heuristics result in a compilation complexity that is quadratic to the number of qubits in the quantum processor (experimentally observed in Figure 12).

Hardware modularity adds significant complexity to this already hard task, as inter-chiplet links are typically inferior compared to intra-chiplet ones [22, 45], connectivity across chiplets is often limited [14, 27], and not all basis gates are necessarily supported across chiplets [32]. In fact, popular quantum software stacks today (e.g., Qiskit [20]) are not even cognizant of the existence of hardware modularity. Hardware modularity, though, also presents an opportunity. Inspired by classical compilation, in this paper we leverage hardware modularity to achieve compilation modularity.

Compilation in classical systems is typically performed independently and in parallel for each source file, producing one object file per source. The individual object files are then linked together to construct the executable. We propose a compilation framework for modular quantum processors that works in a similar fashion: it **stratifies**, i.e., splits, the source quantum circuit into subcircuits small enough to fit in each chiplet, and maps subcircuits to chiplets, and then *in parallel* **elaborates** each subcircuit and compiles it for its target chiplet. This **Stratify-Elaborate Quantum Compiler (SEQC)** stratifies a source program only once for a given chiplet architecture, and performs only the elaboration step recurrently before each execution.

As the qubit capacity n of quantum processors grows exponentially, the $O(n^2)$ compilation latency of contemporary compilers rises even faster. SEQC replaces the recurrent $O(n^2)$ compilation step with several parallel $O(k^2)$ elaboration steps for k -qubit chiplets. The stratification step is $O(n^2)$, so the end-to-end complexity remains the same, but stratification is performed only once. The recurrent compilation in SEQC is only $O(k^2)$, and as the number of qubits k per chiplet is expected to remain relatively stable, or grow at a much slower pace in the foreseeable future [18], SEQC’s recurrent compilation latency will barely grow as processors scale.

Additionally, as SEQC is cognizant of hardware modularity, it can stratify the source quantum circuit into subcircuits and map them to chiplets to minimize inter-chiplet communication. As we show in this paper, SEQC produces circuits with shorter execution times and significantly fewer inter-chiplet gates compared to today’s stock compilers, leading to higher execution fidelity. More importantly,

as the number of qubits in a processor grows, SEQC achieves even higher performance in these figures of merit.

In summary, the contributions of this paper are as follows:

- We make stock compilers aware of hardware modularity, thereby allowing them to correctly compile circuits for modular architectures with limited cross-chiplet gate support.
- We design and implement SEQC, a Stratify-Elaborate Quantum Compiler for modular architectures. SEQC performs compilation in two stages, with the first stage (stratification, or chiplet splitting) performed only once for a given architecture, and the second stage (elaboration, or chiplet compilation) performed in parallel for each chiplet. Only this second stage needs to be performed before each execution, and thus SEQC’s compilation time is largely unaffected by the growth of qubit counts in future quantum processors.
- We design and implement in SEQC several novel methods for qubit placement, qubit routing, and circuit optimization. SEQC compiles circuits with 9.3% higher circuit fidelity on average (up to 49.99%), while consistently achieving 3.27× faster compilation time on average (up to 6.74×) compared to a chiplet-unaware Qiskit baseline.

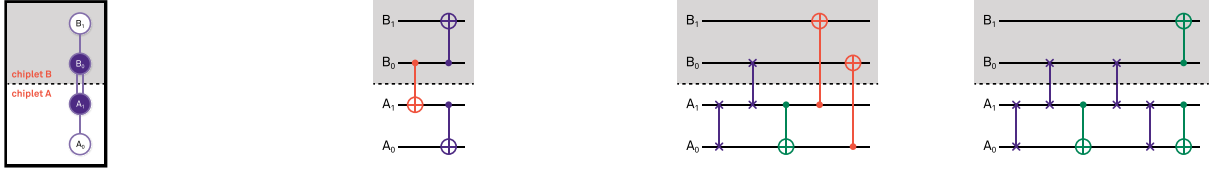
2 Background and Motivation

To execute a program on a target device, the *logical* program representation must be transformed such that it conforms to the idiosyncratic *physical* constraints for that particular device. This process of logical-to-physical translation represents a critical part of compilation and is present even in exotic computing technologies, e.g., quantum. In quantum computing, programs are (usually) represented as *quantum circuits*, and devices are subject to domain-specific physical constraints, such as decoherence time [31], qubit topology (the connectivity between physical qubits) [43, 19], and the set of basis gates (the family of operations physically implemented on the device). Thus, quantum circuit *compilation* is necessary to actually run quantum programs on real-world devices.

Compilation is often divided into distinct stages such as qubit allocation (layout and routing), basis translation, and optimization. The relations between each stage and the physical constraints of both monolithic and chiplet architectures are described below.

Qubit Allocation. Qubit allocation addresses the topology constraints of quantum devices, where physical qubits on a device have limited connectivity to other qubits on the device. It is critical that after this stage, which often requires the modification or addition of circuit gates, the resulting optimized, technology-dependent circuit is functionally equivalent to the original, technology-independent algorithm [44]. The qubit allocation problem has been previously shown to be NP-complete [43]. Thus, algorithms often adopt various strategies to make the problem more tractable. One common method is to further divide qubit allocation into two substages: *layout* and *routing*. Logical-to-physical qubit layout, also known as qubit placement, involves deriving an injective map from the virtual qubits of the quantum circuit to the physical qubits of the quantum device [19, 23]. In other words, the qubit layout stage decides the initial position of logical qubits on the device. In contrast, qubit routing operates from an initial qubit layout and inserts SWAP operations to align a quantum circuit’s gates to a given qubit topology.

¹The term “execution” here includes all shots required to produce a final result for the user. Different executions of the same circuit can span qubit calibration windows.



(a) Example 2-chiplet architecture (b) Input circuit from qubit allocation (c) Insertion of perfect-shuffle (d) Insertion of return SWAPs

Figure 1: Peephole correction for incompatible (non-SWAP) gates placed on inter-chiplet edges. Gates that are unimplementable on hardware are shown in red.

Consider, for example, the state-of-the-art in qubit allocation: the SABRE heuristic search algorithm [23]. In SABRE, the distinction of the layout and routing stages motivates an iterative method for solving qubit allocation. Namely, an initial layout is used to perform qubit routing, which is used to generate a new initial layout.

Because qubit routing remains NP-hard [19], another method of simplifying the problem is to assume qubit links are roughly equivalent, particularly with respect to average fidelity and two-qubit gate duration. This assumption can manifest implicitly when a given device topology is represented as an unweighted, undirected graph. For monolithic architectures, one could debate the marginal tradeoff between performance and solution quality. However, for modular architectures, the cross-chiplet connections are far worse compared to intra-chiplet connections [45]. Thus, we could expect the solutions generated from the simplified model to be worse than a more physically accurate model, for example, in circumstances where the shortest path in terms of the quantity or depth of inserted SWAPs diverges from the shortest path in terms of fidelity, gate duration, or some combination thereof.

Basis Translation. Basis translation converts the gates of an input quantum circuit into gates that are physically supported on hardware. Monolithic quantum architectures typically support a so-called *universal* basis gate set, where any unitary quantum operation can be constructed using solely the gates in the set [31]. Moreover, it has been shown that basis translation can be performed efficiently given the target gate set is universal, and the quantum circuit contains a fixed, finite number of qubits [9]. Unfortunately, modular quantum architectures depend upon specialized links to connect otherwise-independent chiplets. In the general case, the cross-chiplet links can only be used for data movement (such as SWAPs) and not computation, meaning these links may not support universal operations [32]. Thus, compilers that depend on the expectation of universality among qubit links [48], and do not expect these *heterogenous, non-universal* basis gate sets, can generate incompatible outputs when targeting modular architectures.

Optimization. Quantum circuit optimization seeks to prune extraneous operations by finding opportunities to combine, eliminate, and/or parallelize quantum gates [28]. Through commutation and cancellation identities, it is possible to search for optimization opportunities by iteratively transforming the quantum circuit without affecting the underlying operation [28]. However, in general, optimization is highly time and resource intensive, with the problem scaling exponentially with respect to number of qubits and/or circuit depth [21]. As a result, partitioning, the division of a quantum

circuit into *blocks* of quantum gates, is a common tactic among optimization techniques [21, 50, 51]. One major consideration in this process is demarcation, i.e., where and when to draw the line between blocks. Namely, one forfeits all optimization opportunities along boundaries of demarcation, so they must be carefully chosen to minimize the negative impact on the output solution. From this perspective, modular architectures are naturally synergistic with partitioning, since cross-chiplet connections present a physically motivated boundary between operations.

3 Compilation for Modular Quantum Systems

Modular quantum architectures introduce new challenges to quantum compilation that impact the correctness of solutions and the speed of compilation. As discussed previously in §2, our model of modular quantum architectures considers the possibility that inter-chiplet links can be *non-universal*. This is representative of hardware manufacturing constraints [32], where only a restricted set of operations, e.g., state transfers or SWAPs, may be supported over long-distance couplers (inter-chiplet links). However, many compiler designs (including designs for modular architectures, see §7) experience errors or crashes when presented with non-universal, heterogenous, basis gate sets. For example, the Qiskit compiler [20] is explicit in its compatibility for only universal basis gate sets [48]. While it is possible to create a Qiskit Backend that supports heterogeneous basis gate sets, the compiler itself does not take them into account. Specifically, the Qiskit routing stage [53] (an implementation of SABRE) will freely place gates on incompatible physical links, and there are no methods in the compiler to prevent or fix consequent errors. Moreover, compilers are called to target increasingly larger quantum devices, enabled by modularity. To address the mounting pressure of ever-growing compilation workloads, these compilers must be cognizant of classical hardware limitations and tradeoffs between solution quality and compilation latency.

To ameliorate these issues, we present a family of compilers optimized for modular quantum architectures that support chiplet links with non-universal basis gate sets, and leverage modular compilation strategies. In Section 3.1, we propose a peephole compilation pass that can be inserted into *any* compiler to add support for non-universal basis gate sets. This would allow any compiler to be compatible with chiplet-based devices without significant changes to their underlying implementations. Next, in Section 3.2, we introduce the stratify-elaborate quantum compiler (SEQC), which advocates for a hierarchical two-stage compilation that produces both better circuits for execution and faster compilation times.

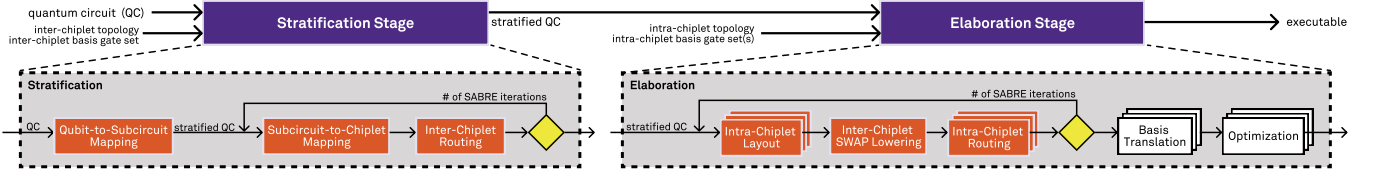


Figure 2: High-level diagram of SEQC. Elements in red reflect modifications from existing compiler designs.

3.1 Chiplet-awareness via Peephole Correction

The design of the peephole correction pass was inspired by the “peephole” optimizations commonly used in classical compilation [2]. Peephole passes operate within a nominal peephole window and substitute its contents with a logically equivalent replacement. Notable examples in the context of quantum compilation include basis translation and elimination of self-adjoint gates. Peephole correction (Figure 1) operates on a circuit generated by qubit allocation, where it detects when non-SWAP gates are placed on non-universal inter-chiplet links (Figure 1b), and employs a cyclic qubit rotation, i.e., a perfect shuffle permutation, to move the aforementioned gates to nearby intra-chiplet links (Figure 1c). Additional “return” SWAPs are then inserted to return the qubits to their initial locations (Figure 1d). Overall, for every inter-chiplet gate in the original circuit generated by SABRE, the peephole pass inserts 4 additional SWAP gates – 2 inter-chiplet and 2 intra-chiplet. Ultimately, this degree of overhead is inevitable when the stock, unmodified compiler is unaware of chiplet-specific device constraints.

For example, skipping the return SWAP operations would initially appear to save 2 SWAPs, thus halving the cost per inter-chiplet gate. However, this hypothetical design would also no longer be a true peephole, since it introduces a net qubit permutation that propagates to downstream gates in the circuit. From the perspective of modular compilation, this results in serial dependencies that prevent parallel execution of the pass. From a routing perspective, the resultant qubit permutations disrupt the post-routing layout of qubits, leading to destructive routing errors that can only be resolved by an entirely new routing pass. Overall, such a hypothetical pass results in substantially worse output circuits compared to the peephole method.

3.2 The Stratify-Elaborate Quantum Compiler

We incorporate the hierarchical elements of chiplet architectures into SEQC by adopting a two-stage procedure (Figure 2). The first, **stratification stage**, represents a one-time overhead to elevate a quantum circuit to the chiplet level. The second, **elaboration stage**, represents a recurring cost to complete the compilation of a quantum circuit given the most up-to-date backend properties.

3.2.1 Stratification Stage. In this stage, we map a quantum circuit to the inter-chiplet device topology (Figure 3a in our running example) by stratifying it into smaller, interconnected *subcircuits*. This can be accomplished with the following intermediate steps (Figures 3b–3d). First, **qubit-to-subcircuit mapping** designates which logical qubits belong to which logical subcircuits. Then, as part of **chiplet allocation**, we define a mapping of logical subcircuits to

physical chiplets on the target device and route inter-chiplet gates to conform with constraints of physical-chiplet connectivity.

Algorithm 1 Qubit-to-Subcircuit Mapping with Sim. Annealing

```

1: procedure COST(Circ, L)
2:    $C \leftarrow 0$  ▷ Count
3:   for  $g \in \text{TwoQubitGates}(\text{Circ})$  do
4:      $q_0, q_1 \leftarrow \text{Qubits}(g)$ 
5:      $s_0, s_1 \leftarrow L[q_0], L[q_1]$ 
6:     Increment  $C$  if  $s_0 \neq s_1$ 
7:   return  $C$ 
8: procedure KICK( $D, N_C, N_Q, L$ )
9:    $L' \leftarrow \text{COPY}(L)$ 
10:  for  $i = 1, \dots, D$  do
11:     $s_0 \leftarrow \text{RANDCHOICE}(\{1, \dots, N_C\})$ 
12:     $q_0 \leftarrow \text{RANDCHOICE}(L'[s_0])$ 
13:     $s_1 \leftarrow \text{RANDCHOICE}(\{1, \dots, N_C\} - \{s_0\})$ 
14:     $q_1 \leftarrow \text{RANDCHOICE}(L'[s_1])$ 
15:    ▷ Swap  $q_0$  and  $q_1$  ◀
16:     $L'[s_0] \leftarrow (L'[s_0] \cup \{q_1\}) - \{q_0\}$ 
17:     $L'[s_1] \leftarrow (L'[s_1] \cup \{q_0\}) - \{q_1\}$ 
18:  return  $L'$ 
19: procedure Q2SMAPPING(Circ,  $N_C, N_Q, T_0, \alpha, \beta$ )
20:   $L \leftarrow \text{Initial Layout}$  ▷ Current Solution
21:   $R \leftarrow L$  ▷ Best Solution
22:   $T \leftarrow T_0$  ▷ Annealing “Temperature”
23:  while  $T > 1$  do
24:     $D \leftarrow \text{CEIL}(T \times \alpha)$  ▷ Number of changes to make
25:     $L' \leftarrow \text{KICK}(D, N_C, N_Q, L)$ 
26:     $\Delta \leftarrow \text{COST}(\text{Circ}, L') - \text{COST}(\text{Circ}, L)$ 
27:     $k \leftarrow \text{RAND}(0, 1)$  ▷ Random number in  $[0, 1) \subset \mathbb{R}$ 
28:     $L \leftarrow L'$  if  $(\Delta < 0)$  or  $(k > \exp(\Delta/T))$ 
29:     $R \leftarrow L'$  if  $(\text{COST}(\text{Circ}, L') < \text{COST}(\text{Circ}, R))$ 
30:     $T \leftarrow T \times \beta$  ▷ Decrease temperature
31:  return  $R$ 

```

Qubit-to-Subcircuit Mapping. Qubit-to-subcircuit mapping produces a *stratified* quantum circuit, where logical qubits (numbers in Figure 3b) are grouped into subcircuits (lowercase letters). An optimal qubit-to-subcircuit mapping minimizes the number of connections between subcircuits, thereby reducing the number of inter-chiplet SWAPs needed to transfer data between chiplets during execution. To perform this task, we investigate two methods: Simulated Annealing and Spatio-Temporal Aware Qubit Allocation (STA) [33].

Simulated annealing is an efficient stochastic optimization technique shown to work well on NP-complete problems, such as place-and-route in VLSI algorithms [41]. Simulated annealing is an iterative method to optimize a state against a given cost function. In each iteration, the state is “kicked,” or randomly perturbed, and the new

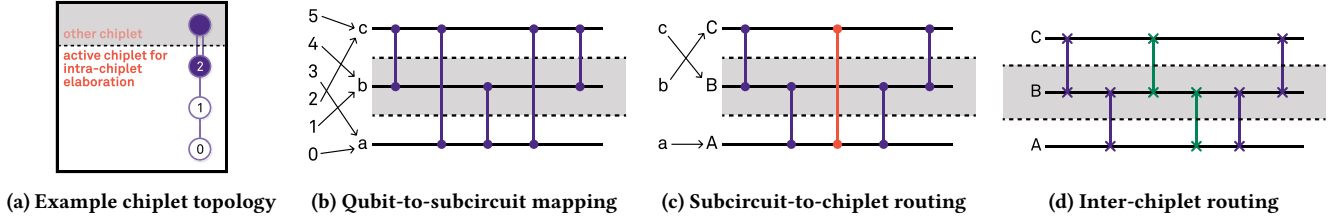


Figure 3: Step-by-step example of inter-chiplet compilation in the Stratification stage.

state is greedily accepted if there is a reduction in cost. However, the algorithm may randomly also accept worse solutions to escape from local minima wells. The runtime of simulated annealing is statically determined using constant tuning parameters, thus the overall complexity is determined by the complexity of the cost and kick functions, which are typically polynomial. Additionally, since each run of a simulated annealing is randomized and independent, it is possible to run multiple trials in parallel with different initial random seeds, then pick the best result. This improves the chances of finding a (near-)optimal solution. Our method is shown in Algorithm 1. We start with an initial qubit-to-subcircuit mapping, which we minimize against a cost function, defined on line 1 as the number of inter-chiplet gates given a certain layout. By minimizing the number of inter-chiplet gates, we implicitly reduce the inter-chiplet connectivity. The kick function then swaps random qubits in the layout, ensuring that each SWAP is between qubits in different subcircuits. In doing so, we hope to move strongly interacting qubits close together, minimizing the number of cross-chiplet gates. As input, our algorithm takes the input circuit $Circ$, the chiplet count N_C , the chiplet size N_Q , the starting temperature T_0 , the number of changes to do per degree of temperature α , and the cooling factor β . The last three are constant tuning parameters across runs.

The STA algorithm is a qubit allocation algorithm designed for trapped-ion quantum systems. These devices often feature modular designs, where one device is composed of “traps” arranged in a (typically) line or ring topology, where each trap contains multiple qubits (ions). Thus, it seems possible to adapt qubit allocation algorithms designed for trapped-ion systems to support modular transmon systems as well. Specifically, one component of STA, denoted as Algorithm 2 in Ovide *et al.* [33], assigns qubits to ion traps, which we can leverage to perform qubit-to-subcircuit mapping and generate an initial subcircuit-to-chiplet mapping.

Chiplet Allocation. Chiplet allocation describes the process of transforming a stratified circuit to be compatible with the inter-chiplet topology of a modular device. In Figure 2, we decompose chiplet allocation into subcircuit-to-chiplet mapping and inter-chiplet routing, analogous to how qubit allocation can be decomposed into qubit layout and routing. Accordingly, subcircuit-to-chiplet mapping (Figure 3c), defines an initial placement of logical subcircuits (lowercase letters) to physical chiplets (uppercase letters). Subsequently, inter-chiplet routing (Figure 3d) inserts inter-chiplet SWAPs to account for limited cross-chiplet gate connectivity.

In our design, we use our qubit-to-subcircuit mapping to provide an initial subcircuit-to-chiplet mapping. Then, we extend and modify the SABRE algorithm [23] to apply to chiplets, placing

Algorithm 2 Inter-Chiplet Routing

```

1: procedure FINDSWAPS( $Q, E$ )
2:   return FINDSYMBIOTICSWAPS( $Q, E$ ) if non-empty
3:   return FINDCOMMENSALISTICSWAPS( $Q, E$ ) if non-empty
4:   return FINDPARASITICSWAPS( $Q, E$ )
5: procedure VALIDGATES( $Q, L$ )
6:   Initialize  $V_{virt}$  and  $V_{phys}$  to empty sets
7:   for  $g \in Q$  do
8:      $H \leftarrow \{L[q] \mid q \in \text{QUBITS}(g)\}$  ▷ Get chiplet info
9:     if  $|H| = 1$  then ▷ All qubits on same chiplet
10:      Add  $g$  to  $V_{virt}$  and  $(g, H)$  to  $V_{phys}$ 
11:   return  $V_{virt}, V_{phys}$ 
12: procedure STEP( $Q, R, L, D$ ) ▷ Advances the “wavefront”
13:    $V_{virt}, V_{phys} \leftarrow \text{VALIDGATES}(Q, L)$ 
14:    $R \leftarrow R + V_{phys}$ 
15:   for  $g \in V_{virt}$  do
16:     Remove  $g$  from  $Q$ 
17:     for  $c \in \text{CHILDREN}(g, D)$  do
18:       Add  $c$  to  $Q$  if  $p \in R$  for all  $p \in \text{PARENTS}(c, D)$ 
19: procedure HEURISTIC( $S, R, Circ$ )
20:    $L' \leftarrow \text{SWAP}(\text{COPY}(L), S)$ 
21:    $C \leftarrow 0$ 
22:   for  $g \in \text{TWOQUBITGATES}(Circ)$  do
23:     if  $g \notin R$  then
24:        $q_0, q_1 \leftarrow \text{QUBITS}(g)$ 
25:        $s_0, s_1 \leftarrow L[q_0], L[q_1]$ 
26:       Increment  $C$  if  $s_0 \neq s_1$ 
27:   return  $C$ 
28: ▷  $L$  is from Algorithm 1,  $T$  is the chiplet topology. ◀
29: procedure INTERCHIPLETROUTING( $Circ, L, T$ )
30:    $D \leftarrow \text{CIRCUITToDAG}(Circ)$ 
31:    $E \leftarrow$  All-pairs distances from chiplet topology  $T$ 
32:    $Q \leftarrow \text{FIRSTLAYER}(DAG)$ 
33:    $R \leftarrow$  empty list
34:   STEP( $Q, R, L, D$ )
35:   while  $Q$  is not empty do
36:      $S \leftarrow \text{FINDSWAPS}(Q, E)$  ▷ SWAP Candidates
37:      $S \leftarrow \arg \min_{s \in S} \text{HEURISTIC}(s, R, Circ)$ 
38:     SWAP( $L, S$ )
39:     STEP( $Q, R, L, D$ )
40:    $D' \leftarrow$  Empty DAG
41:   Append  $g$  to  $D'$  for each  $g \in R$  ▷  $R$  is ordered
42:   return DAGToCIRCUIT( $D'$ )
    
```

iterations of inter-chiplet routing alongside randomized qubit permutations to inform a final subcircuit-to-chiplet mapping. We did explore a design that extended other components of STA to perform subcircuit-to-chiplet mapping on transmon chiplet systems,

but did not produce circuits meaningfully better than this iterative approach and increased compilation time, hence it was abandoned.

Inter-chiplet routing seeks to consolidate the qubits of (non-SWAP) inter-chiplet gates to a single chiplet by inserting inter-chiplet SWAPs into the stratified circuit. For a single two-qubit, inter-chiplet gate, we represent inter-chiplet routing as a shortest-path problem, where the two qubits of the gate correspond to chiplet endpoints in the unweighted inter-chiplet connectivity graph. From the shortest path, we can derive an optimal sequence of SWAPs for routing, where the unweighted path length, or chiplet distance, indicates the length of the SWAP chain. However, in the context of a stratified circuit, composed of multiple inter-chiplet gates, it becomes possible to interleave SWAP chains (i.e., efficiently reorder their execution) to reduce the depth and/or total number of inter-chiplet SWAPs. Like qubit routing, we would expect it to be impractical to derive an optimal solution for this more complex picture of inter-chiplet routing at compile-time. Thus, we employ a similar SWAP selection scheme as SABRE [23], where inserted SWAPs are chosen from a pool of SWAP candidates according to a cost heuristic. For our inter-chiplet routing algorithm, we categorize SWAPs from our candidate pool into three tiers, based on a concept of the “efficiency” of each SWAP, as shown in Algorithm 2.

An inter-chiplet SWAP is considered **symbiotic** if it directly affects two inter-chiplet gates in a “beneficial” manner. In other words, each qubit of a symbiotic SWAP corresponds to a different inter-chiplet gate, where the insertion of the SWAP reduces the chiplet distance score of both gates. In theory, this outcome represents the most efficient possible insertion for a single SWAP, and thus should be the highest-priority case for our greedy inter-chiplet routing cost heuristic. Next, **commensalistic** SWAPs are those that do not “harm,” or increase that chiplet distance, of any directly impacted gates. These SWAPs typically occur when an idle qubit can be used as an ancilla qubit to facilitate the routing of an inter-chiplet gate without affecting other inter-chiplet gates. In certain device topologies, a SWAP acting on the qubits of two inter-chiplet gates can also exhibit commensalistic behavior. Finally, **parasitic** SWAPs act on the qubits of two inter-chiplet gates, where one gate benefits while the other is harmed. Since this variety of SWAPs is actively counterproductive towards a gate, it should be, and likely will be, avoided in most circumstances. However, given a particularly onerous circuit, it may be necessary in such rare instances to break out of a deadlock. For example, clearing one gate may free physical qubits to help route others.

3.2.2 Elaboration Stage. Following the stratification stage, each chiplet can be compiled almost completely independently from one another. More precisely, the compilation process within each chiplet is largely identical to that of a monolithic quantum architecture. The only exception is the presence of inter-chiplet SWAPs, which must be lowered from the chiplet level to the qubit level. Once this assignment is made, these SWAPs must remain fixed and immutable to subsequent compilation stages. Despite this overhead, restricting the task of compilation to a narrower domain of qubits facilitates both parallelization (since each subcircuit can be processed in parallel) and problem size reduction (since there are fewer qubits to consider) of the most computationally intensive compilation stages, namely routing and optimization. To accomplish these

tasks, we divide the elaboration stage into two substages: **qubit allocation** and **parallel basis translation and optimization**. Figure 4 illustrates this with an example of elaboration for a single chiplet (Figure 4a) and its corresponding subcircuit (Figure 4b).

Qubit Allocation. We employ a modified version of SABRE to perform qubit allocation in the elaboration stage. Specifically, we parallelize the SABRE routing algorithm and add constraints to maintain correctness when applied to a stratified quantum circuit with inter-chiplet gates. We also explored a layout pass that used portions of the STA algorithm, but the marginal benefits to solution quality were not worth the 5 – 6× slower elaboration time.

The placement of inter-chiplet gates is a non-parallelizable task (due to cross-chiplet interactions) that strongly influences the layout and routing passes, which could otherwise be fully parallelized across chiplets. To account for this, we introduce a serial stage (Figure 4d) between the parallel layout and routing passes that greedily places gates on the nearest valid inter-chiplet edge. A greedy policy was chosen because inter-chiplet gates have more restrictions on valid placements compared to intra-chiplet gates, while also experiencing substantially higher error rates [45]. Once the positions of the inter-chiplet gates are settled, they must remain fixed, imposing an additional constraint on qubit routing. To promote this behavior in SABRE, we extend its cost heuristic to weigh the device topology by fidelity. This causes higher error links to assume higher costs, discouraging SABRE from moving the high-error inter-chiplet gates. As a result, SEQC achieves better solutions in the common case. However, there is nothing to prevent SABRE from incorrectly modifying any inter-chiplet SWAPs. Thus, we need to impose hard restrictions to ensure correctness. We address this by establishing two disjoint gate sets. One gate set operates strictly within a chiplet. This is the traditional gate set for a monolithic processor. The other gate set is the only one permitted to operate across chiplets, and specifically only implements inter-chiplet SWAPs. By restricting each gate set to its own disjoint part of the overall device topology, we ensure correctness across all cases.

Parallel Translation and Optimization. The remaining compilation stages of basis translation and circuit optimization can be easily parallelized at the chiplet granularity (Figure 4f). Basis translation, in particular, is embarrassingly parallel: gates can be translated independently from each other. Meanwhile, as discussed in §2, optimization algorithms already employ partitioning and parallelization to create tractable subproblems from intractably large circuits, facilitating a smaller problem space, lower memory usage, and faster performance. In modular quantum architectures, we physically motivate partitions through the natural chiplet boundaries, enabling us to reap the same resource and performance benefits of partitioning without compromising on solution quality.

4 Methodology

We evaluate quantum compilers based on the quality of their solutions, their speed of compilation, and their ability to scale to large circuits/devices. To experimentally profile these characteristics, we benchmark a compiler on a suite of quantum circuits, detailed in §4.1, targeting a mock chiplet-based quantum backend,

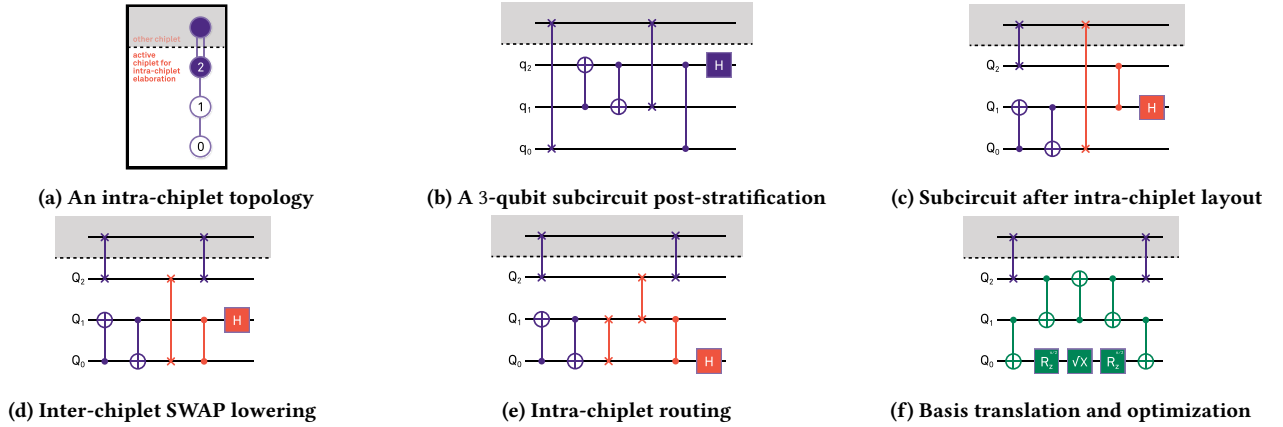


Figure 4: Step-by-step example of intra-chiplet compilation in the Elaboration stage. Gates that cannot be implemented on hardware are shown in red.

as specified in §4.2. In total, we evaluate four compilers—a reference compiler, a peephole-augmented compiler, and two versions of SEQC—on simulated backends ranging from 1 to 100 chiplets. All compilers are implemented in the Qiskit SDK [20] v1.2.4 and Python 3.12.6, and timing results are taken on a machine with a 128-core Ampere Altra Max ARM64 processor and 256 GB of DDR4 RAM. For our reference compiler, we use the one built into Qiskit, parameterized with `optimization_level=3`. Because Qiskit is not natively chiplet-aware, we run these experiments on a backend with *universal* inter-chiplet links (§4.2). To construct the peephole compiler we augment the reference Qiskit compiler by inserting our peephole pass between its routing and `basis_translation` stages, thus making it chiplet-aware. Our two SEQC versions differ in the technique they use for qubit-to-subcircuit mapping. Our first SEQC implementation leverages simulated annealing, initialized with a starting temperature $T_0 = 200$, a rate of change of $0.005T$ per round, $\frac{T}{50}$ permutations per round, and a total of 10 trials per CPU core. Meanwhile, our second SEQC implementation leverages STA for subcircuit-to-qubit mapping and subcircuit-to-chiplet mapping.

We aggregate results in a manner similar to the SPEC family of benchmarks [5], by taking the geometric mean of the relative performance ratio against a baseline technique across a benchmark suite of quantum circuits. The resultant score is then derived for each of the evaluated metrics on multiple backends of varying numbers of chiplets.

4.1 Benchmark Suite

We leverage circuits from Supermarq [47] that are representative of practical, real-world applications for quantum computing, while also being feasible to compile for a large number of qubits. In particular, our suite comprises the following quantum circuits.

Bit Code. Bit codes are often used to detect and correct for bit-flip errors in quantum error correction applications. For an n -qubit benchmark, $k = \lfloor \frac{n+1}{2} \rfloor$ data qubits are prepared in an initial state of $|1010\dots10\rangle$ and fed through two rounds of error correction. The structure of the bit code circuit (Figure 5a) invites many opportunities for gate-level parallelism during compilation. However, because

each logical qubit is connected with its two neighbors with CNOTs, a compiler with an ill-suited topology may struggle to exploit that parallelism due to the number of necessary inserted SWAPs.

Phase Code. Like the bit code, phase codes are often used to detect and correct for phase-flip errors in quantum error correction applications. For an n -qubit benchmark, $k = \lfloor \frac{n+1}{2} \rfloor$ data qubits are prepared in an initial state of $|1010\dots10\rangle$ and fed through two rounds of error correction. To the compiler, the main difference compared to the bit code circuit is the presence of additional single-qubit gates (Figure 5b). This may showcase a compiler’s ability to do noise-aware mapping by differentiating between the relative cost (duration, fidelity) between single- and two-qubit gates.

Greenberger–Horne–Zeiling (GHZ). Entanglement is one of the fundamental properties of quantum states and a major source of quantum advantage. The GHZ state represents a maximally entangled n -qubit state of $\frac{1}{\sqrt{2}}(|0\rangle^{\otimes n} + |1\rangle^{\otimes n})$. The algorithmic circuit structure is essentially a single chain of CNOT gates (Figure 5c) From a compilation perspective, this represents a pure exercise in qubit allocation, because the logical circuit is entirely serial. An n -qubit GHZ circuit that fully utilizes a k -chiplet device should necessitate $\lfloor \frac{n}{k} \rfloor - 1$ logical CNOT operations to extend between chiplets. In turn, this will necessitate at least $2 \left(\lfloor \frac{n}{k} \rfloor - 1 \right)$ inter-chiplet SWAPs to transfer qubit in and out of a chiplet.

VQE. The variational quantum eigensolver (VQE) [37] is another hybrid quantum-classical variational algorithm that is often used in chemistry applications. In our experiments, we choose a 2-layer ansatz whose parameters are again randomly generated (Figure 5d). The resultant circuit structure features two CNOT chains separated by single-qubit operations. The CNOT chains can be interleaved, which in conjunction with the single-qubit gates, creates many opportunities for parallelism (resembling pipelining in classical computing). Moreover, from a qubit routing perspective, the second CNOT chain forces the compiler to consider how qubit permutations in one circuit layer propagate to future layers.

Hamiltonian Simulation. Quantum devices are naturally well-suited to simulating Hamiltonians. The Supermarq benchmark selects the 1D Transverse Field Ising Model (TFIM) system to model,

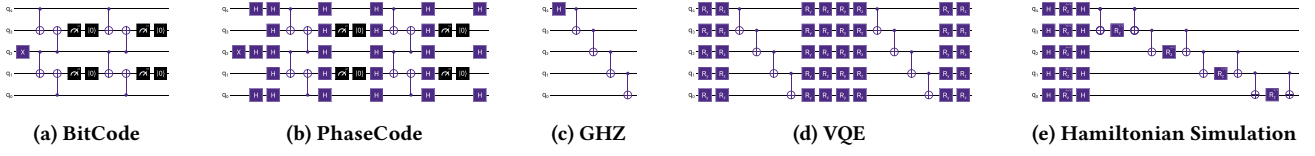


Figure 5: Examples of benchmark applications for 5-qubit circuits.

which is relevant for phase transitions in magnetic materials. The circuit for Hamiltonian Simulation (Figure 5e) resembles a slightly more complex GHZ circuit, including how it is completely serial. Compared to GHZ, this circuit should test the compiler’s ability to lookahead during routing to detect back-to-back gates on the same two-qubit pair, while also emphasizing parallelism originating from the efficient placement of SWAP gates.

4.2 Simulated Quantum Device Specifications

We perform our experiments on mock backends that are generated to conform to the chiplet architecture proposed in Smith *et al.* [45]. The hardware specifications of the qubits and intra-chiplet connections are sourced from Acharya *et al.* [1]. Table 1 details the full specifications. To generate the expected fidelity of the inter-chiplet SWAPs, we perform a simulated random benchmarking trial and calculate the error rate of a SWAP gate with these backend specifications. Following Smith *et al.* [45], we model *inter*-chiplet SWAPs on this backend with $4\times$ the *intra*-chiplet error rate. Similarly, we approximate the duration of the *inter*-chiplet SWAP gate as $4\times$ the duration of an *intra*-chiplet SWAP.

T1 [1]	20×10^{-6} seconds
T2 [1]	30×10^{-6} seconds
Frequency [1]	6×10^9 Hz

(a) Qubit Properties

Instruction	Duration (ns)	Error
X [1]	25.0	0.109%
SX [1]	25.0	0.109%
$R_z(\phi)$ [1]	0.0	0.000%
CZ (intra-chiplet) [1]	34.0	0.605%
CZ (inter-chiplet) [†]	126.0	2.420%
SWAP (inter-chiplet) [‡]	702.4	10.23%
Reset [1]	500.0	0.186%
Measure [1]	500.0	0.196%

(b) Instruction Properties

[†]Universal gate set only. [‡]Non-universal gate set only.

Table 1: Specifications of Simulated Chiplet Backend.

The simulated device has a grid lattice topology of symmetric chiplet modules, where each chiplet features a heavy-hexagon qubit topology [6] (Figure 6). The intra-chiplet topology is constructed such that the heavy-hex structure is preserved for the global device topology (ignoring chiplet division). The tessellation requirements

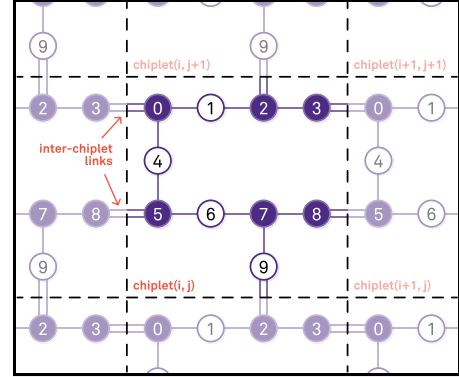


Figure 6: Construction of a grid inter-chiplet lattice from a heavy-hexagon qubit lattice, where the heavy-hex lattice is maintained for each chiplet.

of each chiplet restrict valid chiplet sizes to multiples of 10; however, for our experiments, we limit the size of each chiplet to the minimum of 10 qubits due to hardware limitations. Finally, note that for each valid chiplet count, there may exist multiple valid chiplet topologies. In this work, we generate our backends to use the “most-square” topology for a given chiplet count. For example, a 12-chiplet machine would be generated with a grid of 3×4 chiplets.

5 Experimental Results

We present results for the Qiskit reference compiler, the peephole-augmented Qiskit (PA-Qiskit) compiler, the SEQC compiler using simulated annealing (SEQC-AN), and the SEQC compiler using STA (SEQC-STA). The Qiskit-based and SEQC compilers prioritize different heuristics in compilation. We examine how well each compiler is able to minimize its preferred heuristics, and how well that translates to practical solution quality. Finally, we analyze compilation time, specifically the recurring and non-recurring compilation times for repeating compilations of a single application.

Number of inter-chiplet gates. The primary heuristic we minimize in SEQC is the number of inter-chiplet gates in a quantum circuit. This is because we expect that the inter-chiplet gates of a chiplet architecture contribute the most to error and execution time relative to other gates (at least by a factor of $4\times$ [45]). As a result, the number of inter-chiplet gates should represent a strong proxy metric for the quality of a compiler solution, and thus minimizing the number of inter-chiplet gates should result in higher-fidelity, faster-executing quantum circuits. Accordingly, SEQC consistently produces results that have significantly fewer inter-chiplet gates

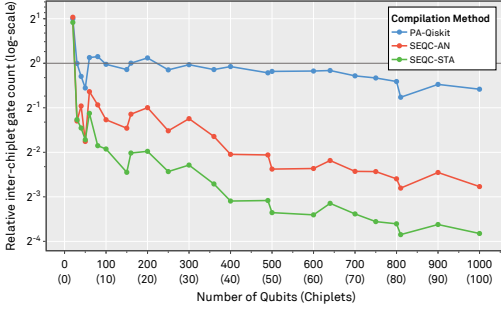


Figure 7: Relative number of inter-chiplet gates for SEQC normalized to the Qiskit baseline (lower is better).

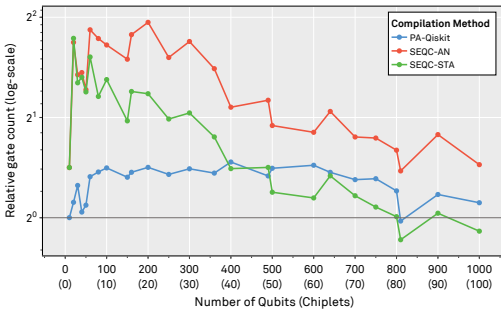


Figure 8: Relative gate count of SEQC normalized to the Qiskit baseline for devices (lower is better).

compared to Qiskit-based compilers (Figure 7). Specifically, compilation with SEQC-STA results in 82.43% fewer inter-chiplet gates on average compared to Qiskit (up to 92.94%). Compared to PA-Qiskit, compilation with SEQC-STA results in 64.92% fewer inter-chiplet gates on average, up to 78.62%. It is worth mentioning that the inter-chiplet gates in the universal backend would be CZ gates, while the non-universal backend would be SWAP gates. For every inter-chiplet (CZ) gate in Qiskit, PA-Qiskit should have 2 inter-chiplet (SWAP) gates. However, we observe PA-Qiskit produces circuits with a roughly comparable number of inter-chiplet gates to Qiskit. In fact, as size increases, PA-Qiskit tends to result in fewer inter-chiplet gates than Qiskit. This outcome may indicate the presence of optimizations that are removing extraneous SWAPs.

Gate count and circuit depth. Gate count and circuit depth are static, backend-agnostic metrics that can serve as indicators for a quantum circuit’s expected fidelity and/or execution time, where circuit depth is the critical path of a quantum circuit in terms of individual gates [31]. SABRE [53, 23], moreover, explicitly minimizes gate count by incorporating it into its cost functions. We observe that SEQC typically produces results with higher gate count and circuit depth compared to Qiskit and PA-Qiskit (Figures 8 and 9). This is due to SEQC prioritizing the reduction of the number of *inter-chiplet* gates over total gate count or circuit depth. Nevertheless, SEQC-STA, in particular, is able to demonstrate competitive results in these metrics for larger circuits. In terms of relative circuit depth, SEQC-STA has comparable or slightly better results compared to

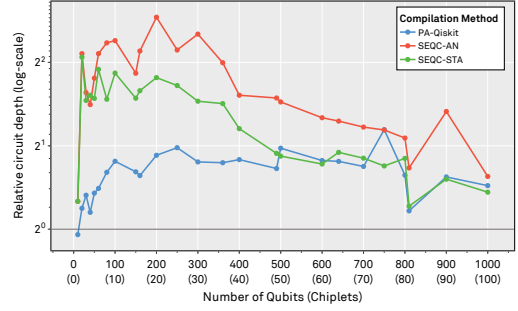


Figure 9: Relative circuit depth of SEQC normalized to the Qiskit baseline for devices (lower is better).

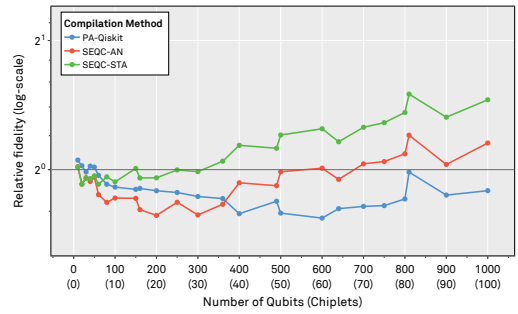


Figure 10: Relative estimated fidelity (ESP) of our proposed compilers normalized to the Qiskit baseline (higher is better).

PA-Qiskit at 500 qubits (50 chiplets) and above. In terms of relative gate count, SEQC-STA has comparable or slightly better results compared to PA-Qiskit at 400 qubits (40 chiplets) and above. For the 810 and 1000 qubit (81 and 100 chiplet) trials, it achieves 14.11% and 8.87% gate count reduction over Qiskit, respectively, despite the latter using universal inter-chiplet links.

Fidelity. Practical applications of quantum computing require some guarantee of program output correctness (measurements). Thus, the highest priority for quantum circuit compilation is to maximize fidelity. Fidelity is impacted by the decoherence constraints of individual qubits, as well as the errors on a gate-by-gate basis [31]. Due to hardware limitations, we were unable to estimate fidelity through simulation. Instead, we leverage estimated success probability (ESP) [39] to approximate fidelity, which can be computed statically. Specifically, we track the per-qubit ESP of a quantum circuit and report an averaged ESP for each benchmark from the geometric mean of the circuit measurements. Figure 10 presents the relative estimated fidelity of each of our compilers compared to the Qiskit compiler with respect to circuit size. There is a noticeable benefit in fidelity associated with the SEQC compiler, particularly with SEQC-STA. We observe an average improvement of 22.13% over PA-Qiskit, up to a 62.87% improvement. Moreover, it is important to mention that the Qiskit trial was ran on a backend with universal inter-chiplet links, which should translate to higher fidelity solutions. Nevertheless, SEQC-STA demonstrates an average improvement of 9.30%, up to a 49.99% improvement.

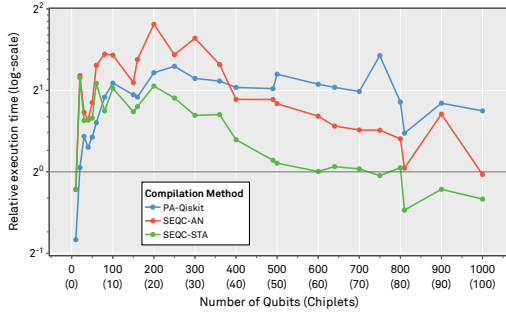


Figure 11: Estimated per-shot execution time of circuits produced by SEQC normalized to circuits produced by the Qiskit baseline (lower is better).

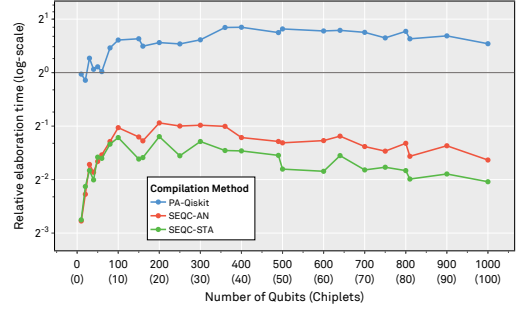


Figure 13: Relative recurring compilation time of our proposed compilers normalized to the Qiskit baseline (lower is better).

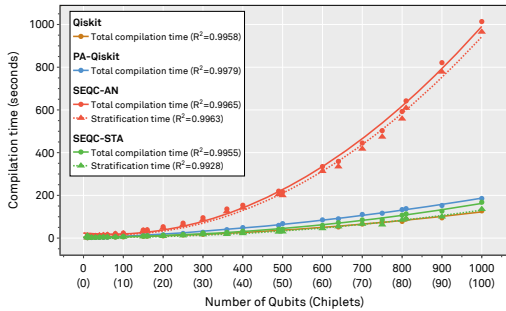


Figure 12: Compilation time of our evaluated compilers (lower is better).

Estimated execution time. The per-shot execution time of a quantum circuit is determined by the critical path of gate operations weighted by gate duration. In addition to performance concerns, execution time indirectly affects fidelity on NISQ-era devices due to decoherence. In other words, it is imperative that quantum circuits execute within the decoherence time to ensure high-fidelity outcomes. Figure 11 presents the estimated per-shot execution time of our proposed compilers relative to the reference as a function of the number of qubits per circuit. As explained previously, we approximate the duration of an inter-chiplot SWAP as $4\times$ the duration of an intra-chiplot SWAP [45]. Under this model, we observe that the SEQC compilers consistently outperform PA-Qiskit in execution by 24.19% on average (63.98% max). It is notable that, despite the gate set affordances given to the Qiskit compiler, SEQC-STA is able to achieve parity in execution time starting from 600 qubits (60 chiplots). For 810 qubits (81 chiplots) and above, SEQC-STA actually compiles faster-executing quantum circuits.

Compilation time. Near-term quantum devices feature rapidly fluctuating error characteristics that can change hourly, or even on a run-to-run basis [46, 30, 8]. Thus, across the entire execution lifetime of an application (quantum circuit), regular re-compilation is necessary to generate the highest-quality circuits with the most up-to-date characteristics possible for every execution. Traditional quantum compilers, like Qiskit and PA-Qiskit, approach each compilation *tabula rasa*, where each new compilation restarts from the

original algorithmic circuit. It is challenging to speed up repeated recompilations without fundamental changes to their design, as noise-aware routing and synthesis algorithms, which leverage updated error characteristics, usually function from a device-agnostic starting point. In contrast, SEQC’s stratification stage enables stateful retention of previous compilations. It is agnostic to the ever-changing error characteristics of a quantum device, and instead only depends on the device’s static topology. Therefore, a stratified quantum circuit can be perennially reused over multiple rounds of compilation, and thus SEQC only repeats the elaboration stage.

Nevertheless, although stratification is a one-time cost for the SEQC compiler, it must be scalable in order to be practical. In Figure 12, we plot the non-recurring compilation time of our evaluated compilers. For our SEQC compilers, we plot stratification time and stratification + elaboration time. These can be compared to the total solve time for the Qiskit and PA-Qiskit compilers. We demonstrate that all compilation times obey a quadratic trajectory ($R^2 \geq 0.9928$).

Figure 13 shows the recurring compilation time. Specifically, this refers to the elaboration time of the SEQC compilers and the full compilation time for Qiskit and PA-Qiskit. Overall, SEQC compilers have a large speedup over Qiskit-based compilers, owing to the use of parallelism and modular compilation strategies. Compared to Qiskit, SEQC-STA achieves $3.27\times$ speedup on average (up to $6.74\times$), and compared to PA-Qiskit $4.69\times$ average speedup ($6.61\times$ max).

6 Discussion

These results demonstrate a flaw with gate count and circuit depth as heuristics: their lack of noise-awareness. Circuit depth and gate count only consider the number of gates (in the critical path and in total) irrespective of each one’s unique underlying properties. It is expected that two-qubit gates will be significantly more noisy than single-qubit gates, and inter-chiplot gates should be significantly more noisy than intra-chiplot gates [45]. Failure to account for duration and error differences between gates or types of gates in quantum compilation heuristics will inevitably result in sub-optimal solutions when the discrepancies are extreme, e.g., in chiplot architectures. Conversely, the hierarchical structure of the SEQC framework with the stratification and elaboration stages imparts some degree of implicit noise-awareness, where minimizing the number of inter-chiplot gates takes precedence over intra-chiplot/total gates.

As a result, SEQC can better optimize for the practically significant metrics of circuit fidelity and circuit execution time.

Overall, we observe that SEQC yields circuits with more desirable characteristics when executing on modular quantum architectures, while at the same time it achieves faster compilation times. Also, as the number of qubits increases, the performance improvement of SEQC widens compared to the baseline, especially for the most important metrics of fidelity, compiled circuit execution time, and number of inter-chiplet gates. These trends hold promise in allowing for faster and better compilation for future large-scale modular quantum devices than we can achieve with today’s frameworks.

7 Related Work

MECH [52] sacrifices some ancillary qubit resources to build an “adjustable multi-entry communication highway” through software. By entangling ancillary qubits and distributing them throughout a chiplet, MECH virtualizes those qubits into fast network-on-chip routing channels. Lin *et al.* [25] present a compilation technique that utilizes calibration data to determine potentially nonstandard 2Q gates that can perform standard operations along bases more compatible with their respective physical states and improve fidelity. Bandic *et al.* [3] utilize the relationship between quantum circuit structure and mapping efficiency to optimize the architecture of monolithic and modular quantum processors, on the path to application-specific hardware optimization. Escofet *et al.* [11] develop a characterization technique for arbitrary quantum circuits which yields theoretical upper and lower optimization bounds, enabling the optimality assessment of qubit mapping solutions. All these techniques are orthogonal to SEQC, and could work synergistically with it to achieve the combined benefits.

CutQC [24] enables smaller-scale quantum computers to execute quantum circuits that are otherwise too large to fit on the device. It partitions large quantum circuits into smaller subcircuits, executes them one at a time, and then merge the individual results at the cost of classical post-processing. Piveteau and Sutter [38] similarly allow subcircuits to execute independently, and use *quasiprobability simulation* to simulate inter-chiplet link behavior where the subcircuits connect, reaching fixed accuracy with less simulation time. SEQC’s stratification stage was inspired by CutQC, but unlike these works SEQC does not perform any classical “stitching” or simulation. It is interesting to note that the first version of SEQC was formulating the problem using constrained optimization as well, but the slowdown of the stratification step was unacceptable and impractical for large quantum circuits, and thus was abandoned in favor of the heuristics we currently employ in our compiler.

Bandic *et al.* [4] map circuit partitioning to min-cut and use the QUBO model with quantum solvers to generate a set of cuts intended to minimize swaps between partitions. QUBO employs quantum optimization algorithms on quantum annealers to accelerate the solution process and remain practical, as the search space for transmission qubits is 2^n . Instead, SEQC takes a “best-effort” approach that works well in practice, and does not require acceleration through quantum means.

Some works on qubit mapping share a few characteristics with SEQC. In a bottom-up approach to qubit mapping, Liu *et al.* [26] partition a circuit into blocks that span an identical number of

qubits, perform permutation-aware synthesis on each block in parallel (solving for all possible qubit topologies), and finally use an augmented SABRE algorithm to map the blocks to the target device and route between blocks. SEQC takes a top-down approach instead, where SWAP permutations between chiplets are settled prior to any compilation tasks performed for each chiplet (block). As a result, SEQC only needs to solve for one qubit layout per block, rather than all permutations. Hungarian Qubit Assignment (HQA) [10] extends the Hungarian algorithm with the ability to adjust a qubit’s cost matrix according to behavior multiple time slices ahead. Pastor *et al.* [36] use deep reinforcement learning to partition quantum circuits for execution across multiple chiplets. Both works aim to reduce inter-chiplet swaps, but assume that all inter-chiplet communications have the same cost, i.e., chiplets are fully connected, which is both impractical for large-scale systems and misses optimization opportunities. SEQC, in contrast, can work with arbitrary chiplet topologies. Ovide *et al.* [34] leverage both quantum and classical methods for inter-chiplet communication to address the scalability challenges of monolithic processors. While it advocates for a two-level, hierarchical approach for quantum circuit mapping, it leaves the actual problem of qubit placement and routing unsolved. SEQC provides an algorithm and implementation, addressing both challenges.

Parallelizing SEQC’s recurrent elaboration step was inspired by traditional classical compilation techniques, which has a decades-long history and is now commonplace [29, 16]. Besides traditional compilation, though, we can also draw parallels between our work and prior research on data movement in the classical space. Data movement is widely understood to be the primary performance bottleneck in the classical architecture space. In the last two decades, work has proliferated on dataflow and spatial architectures, much of which focuses on mapping problems. Consider neural network architectures, for example, which seek to map their physical topologies as closely as possible to problem topologies. Eyeriss [7] approaches the dataflow mapping problem by proposing a row-stationary architecture, and then optimizing the mapping of problem to processing element such that elements which are spatially local in the problem are spatially local in hardware during execution. This is not unlike the target optimization for the stratification stage, and in fact is performed for many of the same reasons — like inter-chiplet swaps, data movements between more distant classical programming elements in a dataflow architecture are more expensive, and minimizing their frequency yields performance improvements.

8 Conclusion

Physical, technological, and economic considerations force future quantum systems to adopt a physically distributed architecture. Modular quantum processors already dominate the roadmaps of several major quantum companies. However, quantum compilers face a scalability challenge brought by the complexity and increasing scale of chiplet-based quantum devices, and their lack of chiplet awareness impedes their ability to produce high-quality results.

In this work, we first modify stock contemporary compilers to become aware of hardware modularity, thereby allowing them to correctly compile circuits for modular architectures with limited cross-chiplet support. We then propose SEQC, a Stratify-Elaborate

Quantum Compiler for modular architectures. SEQC performs compilation in two stages, with the first stage (stratification, or chiplet splitting) performed only once for a given architecture, and the second stage (elaboration, or chiplet compilation) performed in parallel for each chiplet. Unlike contemporary quantum compilers that have to compile a quantum circuit anew before each execution to capitalize on the latest qubit calibration results, only the elaboration stage of SEQC needs to run before each execution. As its computational complexity is a function of the quantum chiplet size, not the entire quantum processor size, and chiplet sizes grow slowly, SEQC's recurrent compilation time is largely unaffected by the relentless growth of qubit counts in future quantum processors.

SEQC implements several novel methods for qubit placement, qubit routing, and circuit optimization, with both hardware modularity and compilation parallelization in mind, achieving on average 9.3% higher circuit fidelity (up to 49.99%), while attaining on average 3.27× faster compilation (up to 6.74×) compared to a chiplet-unaware Qiskit baseline.

Acknowledgements

This research was partially supported by NSF awards CNS-1763743 and CCF-2119069, Academic Year Undergraduate Research Award #2023-17704 by Northwestern University, and undergraduate summer research awards by the Robert R. McCormick School of Engineering and Applied Science and the Computer Science Department at Northwestern University. The authors thank Kabir Dubey for helping with earlier versions of this manuscript.

This research was supported in part through the computational resources and staff contributions provided for the Quest high performance computing facility at Northwestern University which is jointly supported by the Office of the Provost, the Office for Research, and Northwestern University Information Technology.

We acknowledge the use of IBM Quantum services for this work. The views expressed are those of the authors, and do not reflect the official policy or position of IBM or the IBM Quantum team.

References

- [1] Rajeev Acharya et al. 2023. Suppressing quantum errors by scaling a surface code logical qubit. *Nature*, 614, 7949, (Feb. 2023), 676–681. doi: [10.1038/s41586-022-05434-1](https://doi.org/10.1038/s41586-022-05434-1).
- [2] Alfred V. Aho, Monica S. Lam, Ravi Sethi, and Jeffrey D. Ullman. 2006. *Compilers: Principles, Techniques, and Tools (2nd Edition)*. Addison-Wesley Longman Publishing Co., Inc., USA. ISBN: 0321486811.
- [3] Medina Bandic, Pablo le Henaff, Anabel Ovide, Pau Escofet, Sahar Ben Rached, Santiago Rodrigo, Hans van Someren, Sergi Abadal, Eduard Alarcón, Carmen G. Almudever, et al. [n. d.] Profiling quantum circuits for their efficient execution on single-and multi-core architectures. *Quantum Science and Technology*.
- [4] Medina Bandic, Luise Prielinger, Jonas Nüßlein, Anabel Ovide, Santiago Rodrigo, Sergi Abadal, Hans van Someren, Gayane Vardoyan, Eduard Alarcón, Carmen G Almudever, et al. 2023. Mapping quantum circuits to modular architectures with QUBO. In *2023 IEEE International Conference on Quantum Computing and Engineering (QCE)*. Vol. 1. IEEE, 790–801.
- [5] James Bucek, Klaus-Dieter Lange, and J akim v. Kistowski. 2018. Spec cpu2017: next-generation compute benchmark. In *Companion of the 2018 ACM/SPEC International Conference on Performance Engineering (ICPE '18)*. Association for Computing Machinery, Berlin, Germany, 41–42. ISBN: 9781450356299. doi: [10.1145/3185768.3185771](https://doi.org/10.1145/3185768.3185771).
- [6] Christopher Chamberland, Guanyu Zhu, Theodore J. Yoder, Jared B. Hertzberg, and Andrew W. Cross. 2020. Topological and subsystem codes on low-degree graphs with flag qubits. *Phys. Rev. X*, 10, (Jan. 2020), 011022, 1, (Jan. 2020). doi: [10.1103/PhysRevX.10.011022](https://doi.org/10.1103/PhysRevX.10.011022).
- [7] Yu-Hsin Chen, Joel Emer, and Vivienne Sze. 2016. Eyeriss: a spatial architecture for energy-efficient dataflow for convolutional neural networks. In *Proceedings of the 43rd International Symposium on Computer Architecture (ISCA '16)*. IEEE Press, Seoul, Republic of Korea, 367–379. ISBN: 9781467389471. doi: [10.1109/ISCA.2016.40](https://doi.org/10.1109/ISCA.2016.40).
- [8] Samudra Dasgupta and Travis S Humble. 2021. Stability of noisy quantum computing devices. *arXiv preprint arXiv:2105.09472*.
- [9] Christopher M. Dawson and Michael A. Nielsen. 2006. The Solovay-Kitaev algorithm. *Quantum Info. Comput.*, 6, 1, (Jan. 2006), 81–95.
- [10] Pau Escofet, Anabel Ovide, Carmen G Almudever, Eduard Alarc on, and Sergi Abadal. 2023. Hungarian qubit assignment for optimized mapping of quantum circuits on multi-core architectures. *IEEE Computer Architecture Letters*.
- [11] Pau Escofet, Anabel Ovide, Medina Bandic, Luise Prielinger, Hans van Someren, Sebastian Feld, Eduard Alarc on, Sergi Abadal, and Carmen G. Almud ever. 2024. Revisiting the mapping of quantum circuits: entering the multi-core era. (2024). arXiv: 2403.17205 [quant-ph].
- [12] Mark Field, Angela Q. Chen, Ben Scharmann, Eyob A. Sete, Feyza Oruc, Kim Vu, Valentin Kosenko, Joshua Y. Mutus, Stefano Poletto, and Andrew Bestwick. 2024. Modular superconducting-qubit architecture with a multipitch tunable coupler. *Phys. Rev. Appl.*, 21, (May 2024), 054063, 5, (May 2024). doi: [10.1103/PhysRevApplied.21.054063](https://doi.org/10.1103/PhysRevApplied.21.054063).
- [13] Jay Gambetta. 2023. The hardware and software for the era of quantum utility is here. [Accessed 04-14-2024]. IBM, (Dec. 2023). <https://www.ibm.com/quantum/blog/quantum-roadmap-2033>.
- [14] Jay Gambetta and Ryan Mandelbaum. 2024. IBM quantum delivers on performance challenge made two years ago. IBM Quantum Developer Conference (<https://www.ibm.com/quantum/blog/qdc-2024>). (2024).
- [15] Alysso Gold, JP Paquette, Anna Stockklauser, Matthew J Reagor, M Sohaib Alam, Andrew Bestwick, Nicolas Didier, Ani Nersisyan, Feyza Oruc, Armin Razavi, et al. 2021. Entanglement across separate silicon dies in a modular superconducting qubit device. *npj Quantum Information*, 7, 1, 142.
- [16] T. Gross, A. Sobel, and M. Zolg. 1989. Parallel compilation for a parallel machine. In *Proceedings of the ACM SIGPLAN 1989 Conference on Programming Language Design and Implementation (PLDI '89)*. Association for Computing Machinery, Portland, Oregon, USA, 91–100. ISBN: 089791306X. doi: [10.1145/73141.74826](https://doi.org/10.1145/73141.74826).
- [17] HPCWire. 2024. IonQ plots path to commercial (quantum) advantage. Available online at: <https://www.hpcwire.com/2024/07/02/ionq-plots-path-to-commercial-quantum-advantage/>. (July 2024).
- [18] IBM. 2023. IBM debuts next-generation quantum processor & IBM quantum system two, extends roadmap to advance era of quantum utility. Available online at: <https://newsroom.ibm.com/2023-12-04-IBM-Debuts-Next-Generation-Quantum-Processor-IBM-Quantum-System-Two,-Extends-Roadmap-to-Advance-Era-of-Quantum-Utility>. (Dec. 2023).
- [19] Takehiro Ito, Naonori Kakimura, Naoyuki Kamiyama, Yusuke Kobayashi, and Yoshio Okamoto. 2023. Algorithmic theory of qubit routing. In *Algorithms and Data Structures*. Pat Morin and Subhash Suri, (Eds.) Springer Nature Switzerland, Cham, 533–546. ISBN: 978-3-031-38906-1.
- [20] Ali Javadi-Abhari, Matthew Treinish, Kevin Krsulich, Christopher J. Wood, Jake Lishman, Julien Gacon, Simon Martiel, Paul D. Nation, Lev S. Bishop, Andrew W. Cross, Blake R. Johnson, and Jay M. Gambetta. 2024. Quantum computing with Qiskit. (2024). arXiv: 2405.08810 [quant-ph]. doi: [10.48550/arXiv.2405.08810](https://doi.org/10.48550/arXiv.2405.08810).
- [21] Alon Kukliansky, Ed Younis, Lukasz Cincio, and Costin Iancu. 2023. Qfactor: a domain-specific optimizer for quantum circuit instantiation. In *2023 IEEE International Conference on Quantum Computing and Engineering (QCE)*. Vol. 01, 814–824. doi: [10.1109/QCE57702.2023.00096](https://doi.org/10.1109/QCE57702.2023.00096).
- [22] Nicholas LaRacuent, Kaitlin N Smith, Poolad Imany, Kevin L Silverman, and Frederic T Chong. 2022. Modeling short-range microwave networks to scale superconducting quantum computation. *arXiv preprint arXiv:2201.08825*.
- [23] Gushu Li, Yufei Ding, and Yuan Xie. 2019. Tackling the qubit mapping problem for NISQ-era quantum devices. In *Proceedings of the Twenty-Fourth International Conference on Architectural Support for Programming Languages and Operating Systems (ASPLOS '19)*. Association for Computing Machinery, Providence, RI, USA, 1001–1014. ISBN: 9781450362405. doi: [10.1145/3297858.3304023](https://doi.org/10.1145/3297858.3304023).
- [24] Gushu Li, Yufei Ding, and Yuan Xie. 2019. Tackling the qubit mapping problem for nisq-era quantum devices. In *Proceedings of the Twenty-Fourth International Conference on Architectural Support for Programming Languages and Operating Systems (ASPLOS '19)*. Association for Computing Machinery, Providence, RI, USA, 1001–1014. ISBN: 9781450362405. doi: [10.1145/3297858.3304023](https://doi.org/10.1145/3297858.3304023).
- [25] Sophia Fuhui Lin, Sara Sussman, Casey Duckering, Pranav S. Mundada, Jonathan M. Baker, Rohan S. Kumar, Andrew A. Houck, and Frederic T. Chong. 2023. Let each quantum bit choose its basis gates. In *Proceedings of the 55th Annual IEEE/ACM International Symposium on Microarchitecture (MICRO '22)*. IEEE Press, Chicago, Illinois, USA, 1042–1058. ISBN: 9781665462723. doi: [10.1109/MICRO56248.2022.00075](https://doi.org/10.1109/MICRO56248.2022.00075).
- [26] Ji Liu, Ed Younis, Mathias Weiden, Paul Hovland, John Kubiatiowicz, and Costin Iancu. 2023. Tackling the qubit mapping problem with permutation-aware synthesis. In *2023 IEEE International Conference on Quantum Computing and Engineering (QCE)*. Vol. 01, 745–756. doi: [10.1109/QCE57702.2023.00090](https://doi.org/10.1109/QCE57702.2023.00090).
- [27] Ryan Mandelbaum, Antonio D. C orcoles, and Jay Gambetta. 2024. IBM's big bet on the quantum-centric supercomputer: recent advances point the way

- to useful classical-quantum hybrids. *IEEE Spectrum*, 61, 9, 24–33. doi: [10.1109/MSPEC.2024.10669253](https://doi.org/10.1109/MSPEC.2024.10669253).
- [28] Dmitri Maslov, Gerhard W. Dueck, D. Michael Miller, and Camille Negrevergne. 2008. Quantum circuit simplification and level compaction. *IEEE Transactions on Computer-Aided Design of Integrated Circuits and Systems*, 27, 3, 436–444. doi: [10.1109/TCAD.2007.911334](https://doi.org/10.1109/TCAD.2007.911334).
- [29] M. Dennis Mickunas and Richard M. Schell. 1978. Parallel compilation in a multiprocessor environment (extended abstract). In *Proceedings of the 1978 Annual Conference (ACM '78)*. Association for Computing Machinery, Washington, D.C., USA, 241–246. ISBN: 0897910001. doi: [10.1145/800127.804105](https://doi.org/10.1145/800127.804105).
- [30] Prakash Murali, Jonathan M. Baker, Ali Javadi-Abhari, Frederic T. Chong, and Margaret Martonosi. 2019. Noise-adaptive compiler mappings for noisy intermediate-scale quantum computers. In *Proceedings of the Twenty-Fourth International Conference on Architectural Support for Programming Languages and Operating Systems (ASPLOS '19)*. Association for Computing Machinery, Providence, RI, USA, 1015–1029. ISBN: 9781450362405. doi: [10.1145/3297858.3304075](https://doi.org/10.1145/3297858.3304075).
- [31] Michael A. Nielsen and Isaac L. Chuang. 2010. *Quantum Computation and Quantum Information: 10th Anniversary Edition*. Cambridge University Press. doi: <https://doi.org/10.1017/CBO9780511976667>.
- [32] Jingjing Niu, Libo Zhang, Yang Liu, Jiawei Qiu, Wenhui Huang, Jiayang Huang, Hao Jia, Jiawei Liu, Ziyu Tao, Weiwei Wei, et al. 2023. Low-loss interconnects for modular superconducting quantum processors. *Nature Electronics*, 6, 3, 235–241.
- [33] Anabel Ovide, Daniele Cuomo, and Carmen G. Almudever. 2024. Scaling and assigning resources on ion trap qccd architectures. In *2024 IEEE International Conference on Quantum Computing and Engineering (QCE)*. Vol. 01, 959–970. doi: [10.1109/QCE60285.2024.00115](https://doi.org/10.1109/QCE60285.2024.00115).
- [34] Anabel Ovide, Santiago Rodrigo, Medina Bandic, Hans Van Someren, Sebastian Feld, Sergi Abadal, Eduard Alarcon, and Carmen G Almudever. 2023. Mapping quantum algorithms to multi-core quantum computing architectures. In *2023 IEEE International Symposium on Circuits and Systems (ISCAS)*. IEEE, 1–5.
- [35] Alexandru Paler, Daniel Herr, and Simon J Devitt. 2019. Really small shoe boxes: on realistic quantum resource estimation. *Computer*, 52, 6, 27–37.
- [36] Arnau Pastor, Pau Escofet, Sahar Ben Rached, Eduard Alarcón, Pere Barlet-Ros, and Sergi Abadal. 2024. Circuit partitioning for multi-core quantum architectures with deep reinforcement learning. *arXiv preprint arXiv:2401.17976*.
- [37] Alberto Peruzzo, Jarrod McClean, Peter Shadbolt, Man-Hong Yung, Xiao-Qi Zhou, Peter J. Love, Alán Aspuru-Guzik, and Jeremy L. O'Brien. 2014. A variational eigenvalue solver on a photonic quantum processor. *Nature Communications*, 5, 1, (July 2014), 4213. doi: [10.1038/ncomms5213](https://doi.org/10.1038/ncomms5213).
- [38] Christophe Piveteau and David Sutter. 2024. Circuit knitting with classical communication. *IEEE Transactions on Information Theory*, 70, 4, 2734–2745. doi: [10.1109/TIT.2023.3310797](https://doi.org/10.1109/TIT.2023.3310797).
- [39] Fang Qi, Kaitlin N. Smith, Travis LeCompte, Nian-feng Tzeng, Xu Yuan, Frederic T. Chong, and Lu Peng. 2024. Quantum Vulnerability Analysis to Guide Robust Quantum Computing System Design. *IEEE Transactions on Quantum Engineering*, 5, 01, (Jan. 2024), 1–11. doi: [10.1109/TQE.2023.3343625](https://doi.org/10.1109/TQE.2023.3343625).
- [40] Rigetti. 2024. Investor presentation. Available online at: <https://investors.rigetti.com/static-files/fbac3801-223f-4f0f-a207-47d25084a1d7>. (Nov. 2024).
- [41] R.A. Rutenbar. 1989. Simulated annealing algorithms: an overview. *IEEE Circuits and Devices Magazine*, 5, 1, 19–26. doi: [10.1109/101.17235](https://doi.org/10.1109/101.17235).
- [42] SiliconAngle. 2021. Rigetti debuts multichip quantum processor with 80 qubits. Available online at: <https://siliconangle.com/2021/06/29/rigetti-looks-scale-quantum-computing-modular-processor-architecture/>. (June 2021).
- [43] Marcos Yukio Siraiichi, Vinicius Fernandes dos Santos, Caroline Collange, and Fernando Magno Quintao Pereira. 2018. Qubit allocation. In *Proceedings of the 2018 International Symposium on Code Generation and Optimization (CGO 2018)*. Association for Computing Machinery, Vienna, Austria, 113–125. ISBN: 9781450356176. doi: [10.1145/3168822](https://doi.org/10.1145/3168822).
- [44] Kaitlin N Smith and Mitchell A Thornton. 2019. A quantum computational compiler and design tool for technology-specific targets. In *Proceedings of the 46th International Symposium on Computer Architecture*, 579–588.
- [45] Kaitlin N. Smith, Gokul Subramanian Ravi, Jonathan M. Baker, and Frederic T. Chong. 2022. Scaling superconducting quantum computers with chiplet architectures. In *2022 55th IEEE/ACM International Symposium on Microarchitecture (MICRO)*, 1092–1109. doi: [10.1109/MICRO56248.2022.00078](https://doi.org/10.1109/MICRO56248.2022.00078).
- [46] Swamit S. Tannu and Moinuddin K. Qureshi. 2019. Not all qubits are created equal: a case for variability-aware policies for nisq-era quantum computers. In *Proceedings of the Twenty-Fourth International Conference on Architectural Support for Programming Languages and Operating Systems (ASPLOS '19)*. Association for Computing Machinery, Providence, RI, USA, 987–999. ISBN: 9781450362405. doi: [10.1145/3297858.3304007](https://doi.org/10.1145/3297858.3304007).
- [47] T. Tomesh, P. Gokhale, V. Omole, G. Ravi, K. N. Smith, J. Viszlai, X. Wu, N. Haravellas, M. R. Martonosi, and F. T. Chong. 2022. Supermarq: a scalable quantum benchmark suite. In *2022 IEEE International Symposium on High-Performance Computer Architecture (HPCA)*. IEEE Computer Society, Los Alamitos, CA, USA, (Apr. 2022), 587–603. doi: [10.1109/HPCA53966.2022.00050](https://doi.org/10.1109/HPCA53966.2022.00050).
- [48] [n. d.] Translation Errors | IBM Quantum Documentation — docs.quantum.ibm.com. [Accessed 2025-02-20]. %5Curl%7Bhttps://docs.quantum.ibm.com/api/qiskit/qiskit.transpiler.passes.BasisTranslator#translation-errors%7D.
- [49] Rodney Van Meter, Thaddeus D. Ladd, Austin G. Fowler, and Yoshihisa Yamamoto. 2010. Distributed quantum computation architecture using semiconductor nanophotonics. *International Journal of Quantum Information*, 08, 01n02, 295–323. eprint: <https://doi.org/10.1142/S0219749910006435>. doi: [10.1142/S0219749910006435](https://doi.org/10.1142/S0219749910006435).
- [50] Xin-Chuan Wu, Marc Grau Davis, Frederic T. Chong, and Costin Iancu. 2021. Reoptimization of quantum circuits via hierarchical synthesis. In *2021 International Conference on Rebooting Computing (ICRC)*, 35–46. doi: [10.1109/ICRC53822.2021.00016](https://doi.org/10.1109/ICRC53822.2021.00016).
- [51] Ed Younis, Costin C Iancu, Wim Lavrijsen, Marc Davis, Ethan Smith, and USDOE. 2021. Berkeley quantum synthesis toolkit (bqskit) v1. (Apr. 2021). doi: [10.11578/dc.20210603.2](https://doi.org/10.11578/dc.20210603.2).
- [52] Hezi Zhang, Keyi Yin, Anbang Wu, Hassan Shapourian, Alireza Shabani, and Yufei Ding. 2024. Mech: multi-entry communication highway for superconducting quantum chiplets. (2024). arXiv: 2305.05149 [quant-ph].
- [53] Henry Zou, Matthew Treinish, Kevin Hartman, Alexander Ivrii, and Jake Lishman. 2024. Lightsabre: a lightweight and enhanced sabre algorithm. (2024). <https://arxiv.org/abs/2409.08368> arXiv: 2409.08368 [quant-ph].